VOL. 13, NO. 2, JANUARY 2018 ISSN 1819-6608
ARPN Journal of Engineering and Applied Sciences

www.arpnjournals.com

DESIGN AND OPTIMISATION OF DUAL BAND BELL SHAPED FILTER (DBBSF) USING 45° MILTERED BEND AND BUTTERFLY RADIAL STUB (BRS)

Ahmad A.[1] and Othman A. R.[2]
Universiti Teknikal Malaysia Melaka, Centre of Telecommunication and Innovation, Faculty of Electronic and Computer Engineering, Melaka, Malaysia
E-Mail: azmanahmad888@gmail.com

ABSTRACT

A new type of dual-band bandpass filter (BPF) using microstrip line is presented in this paper. The proposed design consists of coupled-lined filter, butterfly radial stub and 45° miltered bending with new structure called Dual Band Bell Shaped Filter (DBBSF). The proposed DBBSF consists of two fundamental resonant modes with the bandwidth resonant characteristic has been investigated using ADS software. The bandwidths are achieved through optimising the butterfly radial stub for high frequency passband. In addition, 45° miltered bend improved its insertion loss and return loss level in good agreement. To validate the design and analysis, the DBBSF were fabricated and measured. The DBBSF leads to reduction of overall circuit size which is 2.5mm x 2.5mm. A dual-band response BPF that operates at 2.4 GHz and 5.75 GHz is designed and implement for wireless applications.

Keywords: dual BPF, dual band bell shaped filter, microstrip coupled-lined, butterfly radial stub, miltered bend.

INTRODUCTION

Development of the dual BPF in RF front-end receiver has received increasing demands for microwave devices. Filter is the important requirement as it acts as a key circuit block in wireless communication systems. Recently, various kinds of methods and techniques to design dual BPFs have been reported. The simplest way to construct a dual-band BPF is combining two single band filters at different passband frequencies (Y. Chen *et al.*, 2006). However, they have the double size and it costly for each single band filter. Another technique such as U-shaped resonators which using only coupling between adjacent resonators without cross-couplings has been presented by Ogbodo E. A. *et al.*, 2016 but the circuit size is still larger. Dual BPF can also be realized by combining two sets of resonators with common input and output (C. Chen *et al.*, 2006). Besides utilizing two or more resonators, a dual BPF can be designed by using a stepped-impedance resonator (SIR) (Zhu H. *et al.*, (2016). Nevertheless, this power capacity of BPF needs to be improved. Another filters reported in coupled-lined section width and gap are so tight from 0.12 ~ 0.13 mm (Mishra A. *et al.*, 2015). Practically, this gap size which is below than 0.5 mm are critical during fabrication process in which high accuracy is essentially needed.

In this paper, an improved dual-band BPF design called Dual Band Bell Shaped Filter (DBBSF) is proposed.Theories and techniques are to be described to extract the parasitic elements in our new model filter. The filter has demonstrates better *S*-parameters and group delay performance as well as compact fabrication size.As shown in Figure-1, the DBBSF structure consists of coupled-lined filter, butterfly radial stub and 45° miltered bending.

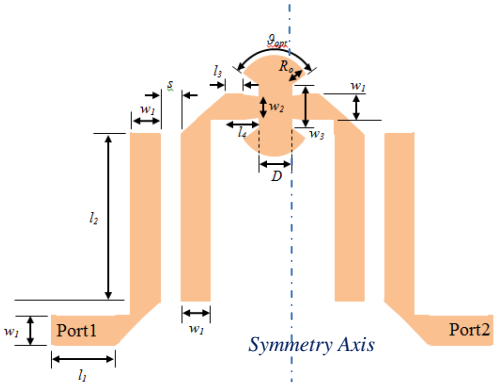

Figure-1. DBBSF design layout.

DBBSF DESIGN AND CONCEPT

The filter is designed on FR4 substrate having a thickness of 1.6 mm, a dielectric constant εr of 4.4, a loss tangent of 0.019 and a thickness copper of 0.035 mm. Choosing the type of filter is the initial process before proceeding to desired design, and then needs a filter specification to achieve goal and target design. Design specifications of the proposed dual BPF are highlighted in Table-1.

Table-1. DBBSF target design specification.

Filter specification	Parameter	
Center frequency	**2.4 GHz**	**5.75 GHz**
Insertion loss (S_{21})	< -10 dB	< -10 dB
Return loss (S_{11})	> -10 dB	> -10 dB
Bandwidth	200 MHz	200 MHz
Attenuation	21 dB @ 1.55 GHz 21 dB @ 3.1 GHz	21 dB @ 4.62 GHz 21 dB @ 6.44 GHz

Initially step to start the construction of DBBSF begin with the simple structure of microstrip parallel coupled lines filter as depicted in Figure-2.

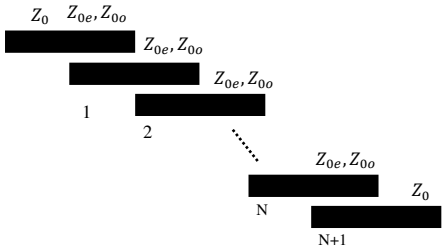

Figure-2. Microstrip coupled-lined layout.

Mathematically, if ω_1 and ω_2 denote the edges of the pass band, then a band pass response can be obtained using the following frequency substitution as equation (1).

$$\omega = \frac{1}{\Delta}\left(\frac{\omega}{\omega_0} - \frac{\omega_0}{\omega}\right) \quad (1)$$

where, Δ is the fractional bandwidth of the pass band can be write as equation (2).

$$\Delta = \frac{\omega_2 - \omega_1}{\omega_0} \quad (2)$$

and the center frequency, ω_0 could be chosen as the arithmetic mean of ω_1 and ω_2, it is specify by equation (3).

$$\omega_0 = \sqrt{\omega_1 \omega_2} \quad (3)$$

After know the n-order filter, the ladder network for low pass filter prototype can be design by referring the table of element value (G. L. Matthaei *et al.*, 1980). The element values are numbered from g_0 at the generator impedance to g_{N+1} at the load impedance for a filter having N reactive elements. The element value is used to design the low pass filter prototype via ladder network. The ladder network has lumped circuit elements consists of shunt capacitors and series inductors. This ladder network has two types which can be design beginning with shunt element or series element as shows in Figure-3.

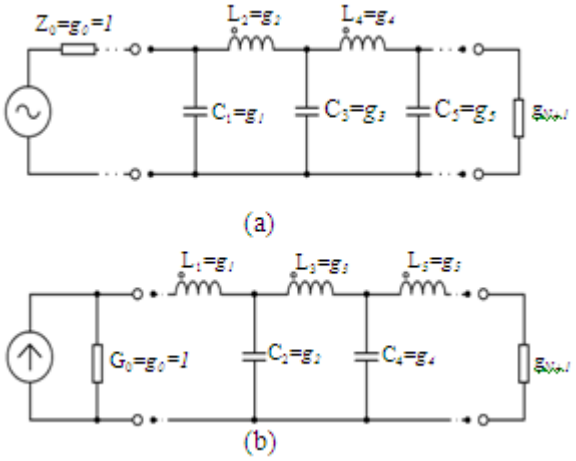

Figure-3. Low pass filters prototypes and their element definitions: (a) Prototype beginning with a shunt element and (b) Prototype beginning with a series element.

For basic conventional bandpass filter design, *J*-inverter concept is used to convert from low pass filter to bandpass filter after obtaining the low pass prototype element values. Finally, the characteristic impedances and dimension of the coupled lines can be attained. After obtaining the low pass prototype element values, external quality factor are calculated using (4) and coupling coefficients using (5).

$$Q_{e1} = \frac{g_0 g_1}{\Delta} \quad , \quad Q_{en} = \frac{g_N g_{N+1}}{FBW} \quad (4)$$

$$M_{i,i+1} = \frac{\Delta}{\sqrt{g_i g_{i+1}}} \quad , \quad for\ i = 1\ to\ N-1 \quad (5)$$

The total length of a coupled line filter with λ/2 straight microstrip line resonator is too much long and the size increases with the order of the filter. To solve this problem, a conventional U-shaped of half of λ/2 length structures were developed as shows in Figure-4(a). Further size reduction is made possible by coupling two arms of L-shaped to form a pair of openly coupled lines of open end arms as shows in Figure-4(b).

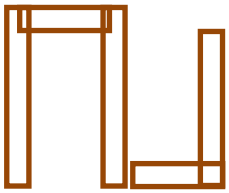

Figure-4. Basic filter structure: (a) U-shaped of half of λ/2 length structure and (b) L-shaped single-sided coupled fed structure.

The length of the U-shaped resonator is half wavelength long. The guided wavelength can be calculated using equation (6). According to Figure-1, the length of U-shaped resonator is 14 mm, which is λ/2. The width of the resonator is 1 mm to match the 50 Ω line. The separation is chosen to be 1 mm.

$$\lambda_g = \frac{300}{f\sqrt{\varepsilon_{re}}} mm \quad (6)$$

Then, the U-shaped was integrated with the butterfly radial stub at the centered of the structure. The element stub useful to provide the output performance by varying the ϑ angle, so it can vary the return loss and consequently the insertion loss for the high frequency band. The electrical performances of the filter are described in terms of insertion loss, return loss, frequency selectivity or attenuation at rejection band, and group delay variation in pass band (Duraikannan, S. *et al*., 2013). The group delay of this bandpass filter can be calculated as mentioned in equations (7), (Lahcen *et al*., 2016).

$$\tau = \frac{-\partial \angle S_{21}}{\partial \omega} \quad (7)$$

where $\angle S_{21}$is the insertion loss phase and ω the frequency in radians per second.

Optimisation of butterfly radial stub

Butterfly radial stub (BRS) has been widely used in many microwave circuits such as filters, matching networks, bias lines even grounding RF signal. According to DBBSF structure in Figure-1, the BRS is connected parallel to the transmission path. The geometry of BRS is based on the combination of two radial stubs as shown in Figure-5(a). In Figure-5(b), the ends of the feed lines are referenced to the center of the radial stub. The penetration depth (P) may exceed the width of the microstrip feed line. The width of the stub base (W) and P are related by the formula as equation (8).

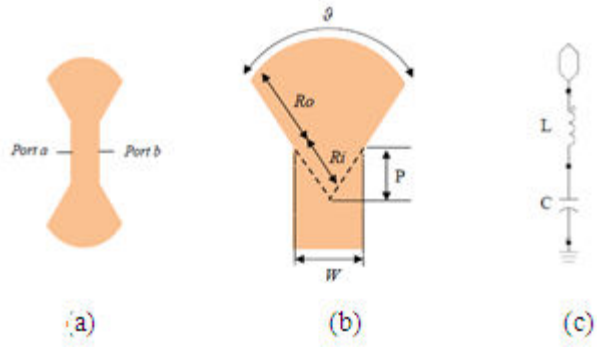

Figure-5. Microstrip radial stub. (a) Butterfly radial stub. (b) Radial stub. (c) Equivalent circuit of (b).

$$W = 2 \times P \times tan\left(\frac{\vartheta}{2}\right) \quad (8)$$

The angle, ϑ is limited to a range from ϑmin<ϑ< 170° due to avoids geometries sizes which do not make sense. From Figure-3(c), the variation of inductance, *L* and capacitor, *C* circuit also can be observed and it depends on the dielectric substrate and mainly on *Ro* and ϑ as mentioned in equations (9) & (10), (March *et al*., 1985).

$$L = \frac{120\pi h}{\vartheta}\left[In\left(\frac{Ro}{Ri} - \frac{1}{2}\right)\right] H \quad (9)$$

$$C = \frac{\vartheta Ro^2 \varepsilon_{eff}}{240\pi hc} F \quad (10)$$

A BRS is an open circuit stub realized in radial transmission line instead of straight transmission line. It is a very useful element, primarily for providing a clean (no spurious resonances) broadband short circuit, much broader than a simple open circuit stub. It is especially useful at high frequencies model. Figure-6 shows the optimizing of the value ϑ at 5.75 GHz.

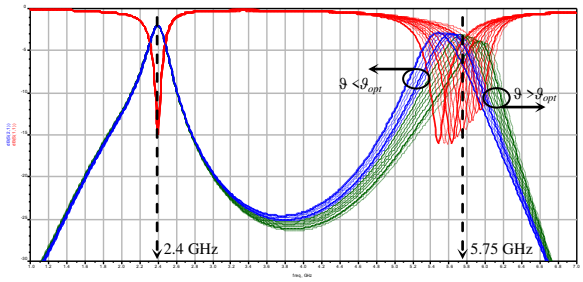

Figure-6. Optimising S_{11} and S_{21} by tuning ϑ value from butterfly radial stub.

According to the Figure-6, when ϑ is less then ϑ_{opt}, the frequency resonance (S_{21}) at the high frequency band is shift to the left, if ϑ is large then ϑ_{opt}, the frequency resonance is shift to the right. The ϑ value decrease or increase by interval 1° to show the effectiveness of the filter performance. The S_{11} also keep tracking respectively when S_{21} are shifted. Based on the result, it also found that the low frequency responses (2.4 GHz) remain at the

initial condition without any changes. It shows that the high frequency can be varied and the low frequency is lock from amendment. As mentioned before, the ϑ should not over than 170° as to ensure the geometries size which do not make sense.

Bend types analysis

There are several types of bend configuration such as curved bend, 45° mitered bend, and 90° bend have been chosen and tested for use in the filter design. Each bending is connected to a 50 Ω input and output transmission line. As shown in Figure-7, each bending type has been plotted by simulating the S_{11} and S_{21} outputs for comparison.

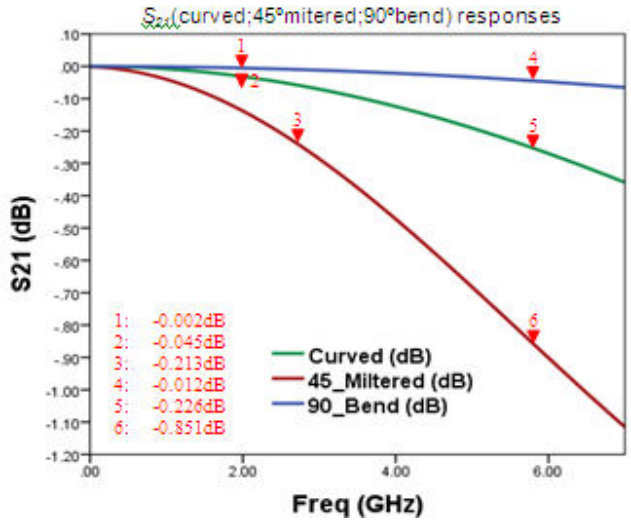

(a)

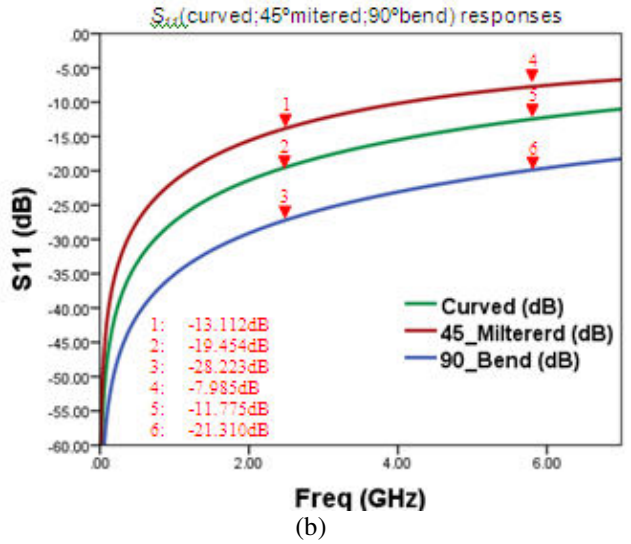

(b)

Figure-7. Simulated three types of bending (curved bend, 45° mitered bend, 90° bend) with 50 Ω input and output transmission line: (a) Insertion loss, S_{21} and (b) Return loss, S_{11}.

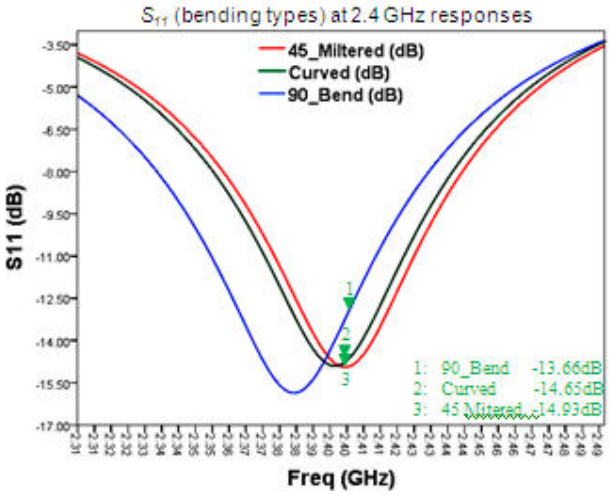

(a)

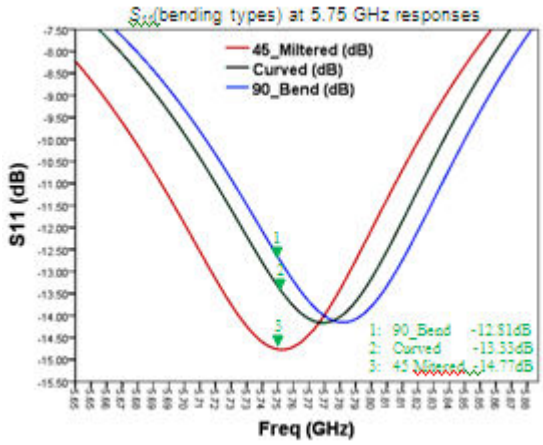

(b)

Figure-8. Simulated S_{11} frequency response of DBBSF with three types of bending: (a) 2.4 GHz and (b) 5.75 GHz.

Among the three different types of bending, it proven that the 45° mitered bending produces the best output for S_{11} and S_{21}. As depicted in Figure-7(a), the $S_{21}$for the curved bend has lessened by 0.168 dB at 2.4 GHz and 0.625 dB at 5.75 GHz compared to the 45° mitered bend. For S_{11}, the bending curved has lessened by 6.342 dB at 2.4 GHz and 3.79 dB at 5.75 GHz compared to the 45° mitered bend as shown in Figure-7(b). The 90° bend also shows that the S_{21} output has lessened by 0.211 dB at 2.4 GHz and 0.839 dB at 5.75 GHz bands compared to the 45° mitered bend as depicted in Figure-7(a). While for S_{11}, the 90° bend has lessened by 6.342 dB at 2.4 GHz and 3.79 dB at 5.75 GHz compared to the 45° mitered bend as shown in Figure-7(b).

Apart from conducting the above simulations, another simulation was implemented on the DBBSF using the same bending types. Figure-8(a) and (b) show the simulation output of S_{11} at 2.4 GHz and 5.75 GHz bands. From Figure-8(a), the S_{11} at 2.4 GHz for curve bend and 45° mitered bend slightly vary between each other and the 90° bend delivers the poorest output compared to others.

Meanwhile in Figure-8(b), the S_{11} at 5.75 GHz clearly shows that the 90º bend delivers poor S_{11} output compared to others. The analysis exhibits excellent transmission notch at 2.4 GHz and 5.75 GHz for the 45º mitered bend type.

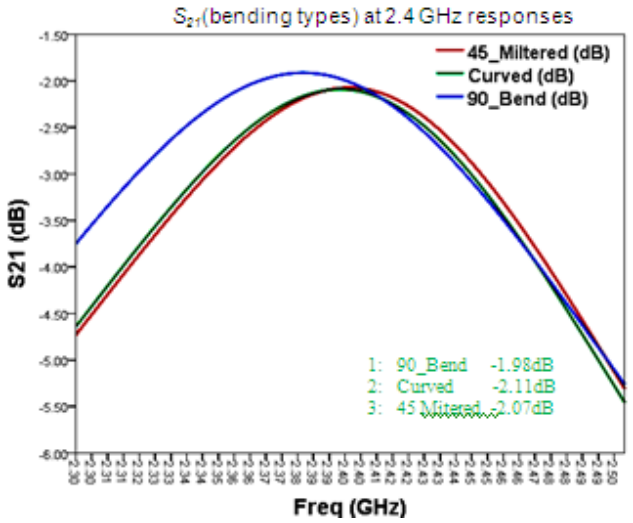

(a)

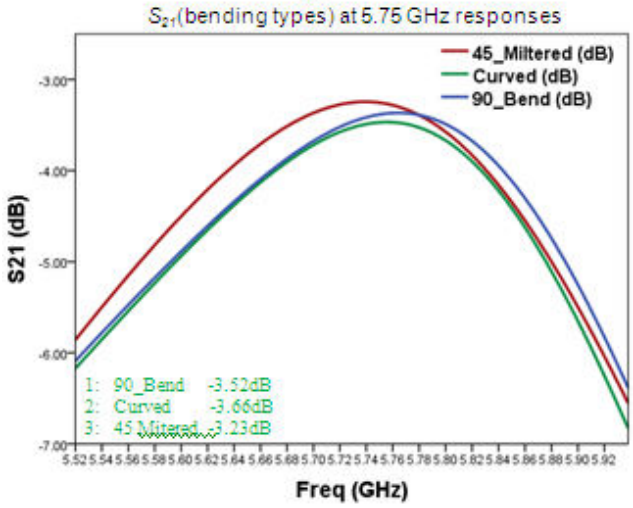

(b)

Figure-9. Simulated S_{21} frequency response of DBBSF with three types of bending: (a) 2.4 GHz and (b) 5.75 GHz.

Figure-9(a) and (b) show the responses of different types of bending at 2.4 GHz and 5.75 GHz for S_{21} parameter using the DBBSF. According to Figure-9(a), the S_{21} at 2.4 GHz output shows that the 45º mitered bend produces the best output compared to others. The output result is -2.07 dB. While at 5.75 GHz, the best output for S_{21} is the 45º mitered bend as depicted in Figure-9(b). By observing the S_{11} and S_{22}simulation results at 2.4 GHz and 5.75 GHz bands, the 45º mitered bend is chosen for use in the DBBSF design because it has the most efficient output compared to others.

Table-2 tabulates the overall performance and simulation results for the S_{11} and S_{21} using three bending types based on Figure-8 and Figure-9.

Table-2. Summary of S_{11} and S_{21} for Figure-8 and Figure-9.

Bending Type	**Max. Return loss, S_{11} in passband** (dB)		**Max. Insertion loss, S_{21} in passband** (dB)	
	2.4GHz	5.75GHz	2.4GHz	5.75GHz
45° Mitered	–14.93	–14.77	–2.07	–3.23
90°	–13.66	–12.81	–1.98	–3.52
Curve	–14.65	–13.33	–2.15	–3.66

Miltering bend is one of the ways in which the reflections can be reduced. A 90° bend in a transmission line adds a small amount of capacitance to the transmission line, which causes a mismatch. A mitered bend reduces some of that capacitance, restoring the line back to its original characteristic impedance. Figure-10 shows the 45° miltered bend. A good example (Hsieh *et al*., 2003) was verified of new parameter in ring resonator with improved *S*-parameters. The ring resonator was 45° miltered bend and simulated to optimize its resonant frequency.

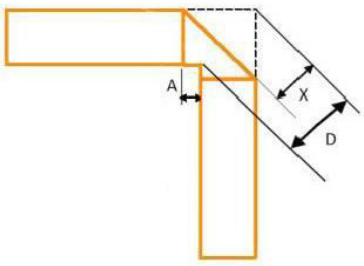

Figure-10. 45° miltered bending.

In DBBSF, the microstrip coupledline was match with butterfly radial stub to provide two resonant at high and low frequency. The termination of 50Ω feeder and the coupled-lined was link by discontinuity of 45° miltered bend. It found that the 45° miltered bend provide a maximum bandwidth of the S_{21} and excellent S_{11} compare to others bending types, (Razalli *et al*., 2008). Figure-11 shows the DBBSF is design in symmetrical, thus all parasitic elements can be extracted from only one side of the equivalent circuit. *L* and *C* are the parasitic elements (bending circuit),*l* and *w* are line width of stub, connecting transmission and feeder.

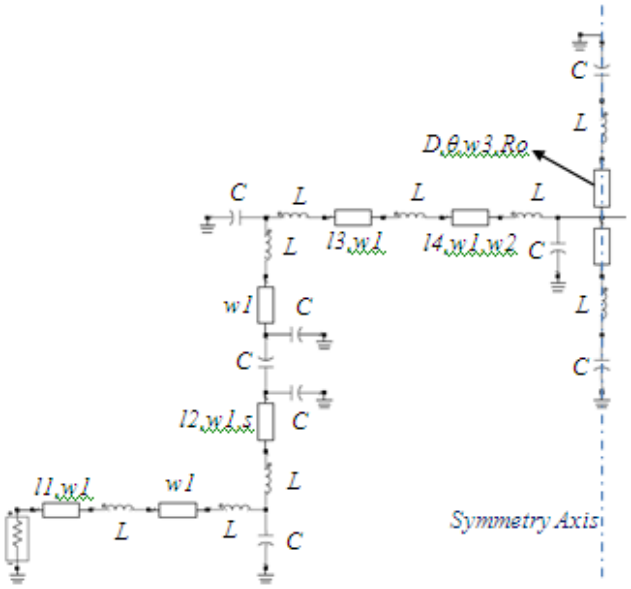

Figure-11. Equivalent circuit (half) for DBBSF.

The physical dimensions of the proposed DBBSF resonator as shown in Table-3. Each dimension at the left side is equals with the right side of symmetry axis. The length and width has been optimized with ranges of 0.5 mm to 14 mm. It should be noted that the parameter ϑ_{opt}(69.9°) is chosen from BRS for adjustable the high band resonance.

Table-3. Dimension of DBBSF with reference to the layout (Figure-1) and equivalent circuit (Figure-7).

Dimension		Item for
***l*1**	**7mm**	**50Ω feeder microstrip length**
*l*2	14mm	Coupled-line length
*l*3	0.5mm	Microstrip length
*l*4	1mm	Taper microstrip length
*w*1	1mm	Microstrip width
*w*2	0.5mm	Taper microstrip length
s	1 mm	Separation gap
ϑ	69.9°	Butterfly radial stub
*w*3	2 mm	
Ro	2.21 mm	
D	1.21 mm	

DBBSF SIMULATION AND MEASUREMENT RESULT

The simulations and measurement graph for DBBSF is depicted in Figure-12. The simulated results show thatS_{21} is –2.07 dB and -3.26 dB and $S_{11}$is –14.9 dB and –14.7 dB at 2.4 GHz and 5.75 GHz respectively. It is seen that the filter has a bandwidth of 220 MHz within frequency from 2.28 GHz to 2.5 GHz and 440 MHz within frequency from 5.49 GHz to 5.93 GHz at -3 dB of the peak response. The design measured using PNA-X Network Analyzer from Agilent Technologies. The measured output of $S_{21}$is -2.13 dB and -3.38 dB and $S_{11}$is -23.3 dB and -19.3 dB at 2.4 GHz and 5.75 GHz respectively. Both bandwidths measured within -3 dB of the response at its peak and obtained 223 MHz and 448 MHz at 2.4 GHz and 5.75 GHz.

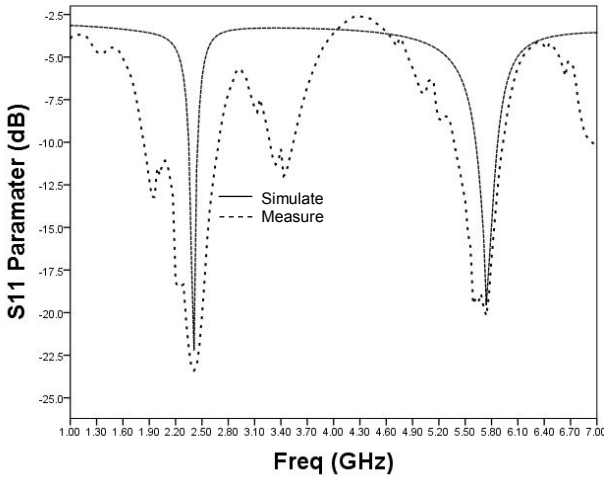

(a)

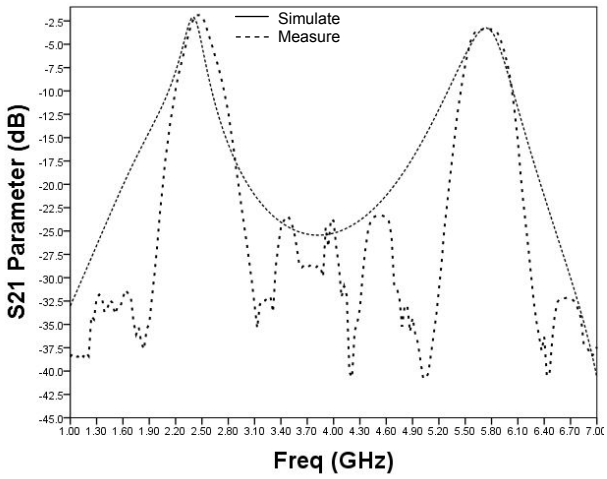

(b)

Figure-12. Simulation and measurement frequency response of DBBSF: (a) $S_{11}$and (b) S_{21}.

Figure-13 shows the DBBSF of group delay simulated and measured. From simulated results, the varies between high and low frequency group delay can be determine with 1.83 ns and 1.23 ns from midband frequency group delay at 0.18 ns. The measured achieved of 1.74 ns and 1.07 ns at respectively bands. A measurement shows how much a device causes these frequency components to become misaligned.

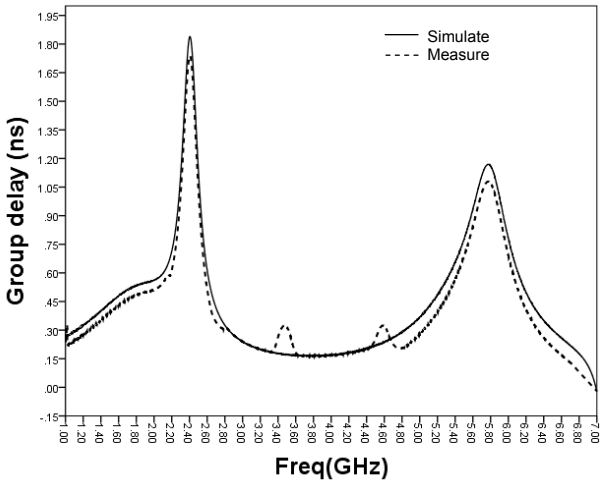

Figure-13. Simulated of group delay for DBBSF.

The filter fabrication is realized by using standard photolithography process on FR4 substrate microstrip. The advantages of microstrip technology include simple, small size, light weight and durable finish as compared to conventional design (Ahmad *et al.*, 2015). These advantages are significant to smaller size RF components design, nowadays.The fabricated prototype of this DBBSF is depicted in Figure-14. Two 50Ω terminal lines are extended to accommodate the SMA connectors to connect to the Vector Network Analyzer (VNA) for measurement. This prototype filter with a small compact size of 2.5 cm x 2.5 cm.

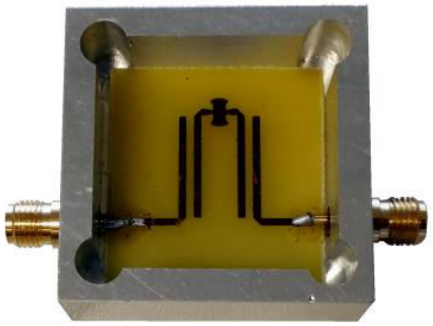

Figure-14. Photograph of the fabricated circuit.

Both simulation and measurement achieved the target requirements. Table-4 shows the comparison of simulation and measurement parameters for DBBSF. By comparing the measurement with the simulation bandwidth results, the differences are 1.36% for 2.4 GHz and 1.81% for 5.75 GHz.

Table-4. Simulated and measured results.

Parameter	Simulation		Measurement	
Frequency (GHz)	2.4	5.75	2.4	5.75
Bandwidth (MHz)	220	440	223	448
Insertion loss, S_{21}(dB)	-2.07	-3.26	-2.13	-3.38
Retun loss, S_{11} (dB)	-14.9	-14.7	-23.3	-19.3
Group delay (ns)	1.83	1.23	1.74	1.07
Attenuation	21 dB @ 1.52 GHz, 21 dB @ 4.26 GHz	21 dB @ 5.26 GHz, 21 dB @ 6.52 GHz	21 dB @ 1.77 GHz, 21 dB @ 3.02 GHz	21 dB @ 5.27 GHz, 21 dB @ 6.19 GHz

CONCLUSIONS

In this paper, Dual Band Bell Shaped Filter (DBBSF) with utilizing transmission of microstrip-lined, butterfly radial stub and 45° miltered bends technique is designed. With the support of the discontinuity 45° mitered bend and BRS could help to reduce the length and improves the aspect ratio of the microstrip size up to 35% - 45% of the size of the conventional coupled-lined bandpass filter. This filter provides us to achieve better S_{11} and S_{21} at the resonant bands of 2.4 GHz and 5.75 GHz. The experimental verification also gives comparison, how close the simulation results and measurements look like. This project contribution to build a part of the dual-band concurrent RF front-end receiver with a dual channels output.

ACKNOWLEDGEMENT

The authors would like to express their acknowledgment to the Centre of Telecommunication and Innovation (CETRI) for supporting this project.

REFERENCES

A Ahmad, AH Hamidon, AR Othman, K Pongot. 2015. A 100 MHz 4 channels Narrow-band Chebyshev Filter for LTE Application. International Journal of Engineering and Technology. 6(6): 2747-2755.

C. Chen and C. Hsu. 2006. A simple and effective method for microstrip dual-band filters design. IEEE Microwave and Wireless Components Letters. 16(5): 246-248.

C.-Y. Chen and C.-Y. Hsu. 2006. A simple and effective method for microstrip dual-band filters design. IEEE Microw. Wireless Compon. Lett. 16(5): 246-248.

Duraikannan S. and Awadh M.S. 2013. Design optimization for diminution of 5.75 GHZ Chebyshev bandpass filter. 2013 IEEE International Conference on Circuits and Systems (ICCAS), pp. 96-101.

G. L. Matthaei, L. Young, and E. M. T. Jones. 1980. Microwave Filters, Impedance-Matching Networks, and Coupling Structures, Artech House, Dedham, Mass.

Hsieh, L. H. and K. Chang. 2003. Compact, low insertion-loss, sharp rejection, and wide-band microstrip bandpass filters. IEEE Transactions on Microwave Theory and Techniques. 51(4): Part 1, 1241–1246.

LahcenYechou, AbdelwahedTribak, Mohamed Kacim, Jamal Zbitou and Angel Mediavilla Sanchez. 2016. A Novel Wideband Bandpass Filter Using Coupled Lines and T-Shaped Transmission Lines with Wide Stopband on Low-Cost Substrate. Progress in Electromagnetics Research C. 67: 143-152.

M. S. Razalli, A. Ismail, and M. A. Mahdi. 2008. Novel compact microstrip ultra-wideband filter utilizing short-circuited stubs with less vias. Progress In Electromagnetics Research, PIER 88, 91-104.

Mishra A. and Gupta R. 2015. Design of a UWB band pass filter based on resonator structure. 2nd International Conference on Electronics and Communication Systems (ICECS), Coimbatore. pp. 1066-1070.

Ogbodo E. A., Wang Y., and Yeo K. S. K. 2016. Microstrip dual-band bandpass filter using U-shaped resonators. Progress in Electromagnetics Research Letters. 59: 1-6.

S. L. March. 1985. Analyzing lossy radial-line stubs. IEEE Trans. Microwave Theory & Tech. MTT-33(3): 269-271.

Zhu H. and Abbosh A. M. 2016. Single- and dual-band bandpass filters using coupled stepped-impedance resonators with embedded coupled-lines. IEEE Microwave and Wireless Components Letters. 26(9): 675-677.